The series $Os_4(\mu_x\text{-}\eta^2\text{-}C_2Ph_2)(CO)_{14-n}$ (n = 0, 1, 2; x = n + 2) — Models for site-specific surface catalysts[1]

John P. Canal, Michael C. Jennings, Glenn P.A. Yap, and Roland K. Pomeroy

Abstract: The cluster $Os_4(\mu\text{-}\eta^2\text{-}C_2Ph_2)(CO)_{14}$ (**1**) has been prepared from the reaction of $Os_4(CO)_{14}$ and C_2Ph_2 in CH_2Cl_2 at 25 °C. Other minor products include the known clusters $Os_3(\mu_3\text{-}\eta^2\text{-}C_2Ph_2)(CO)_{10}$ and $Os_3(\mu\text{-}\eta^4\text{-}C_4Ph_4)(CO)_9$. The structure of **1** reveals an approximately planar C_2Os_4 skeleton with a dimetallacyclobutene ring (C—C = 1.32(4) Å) and a flat butterfly Os_4 unit (Os—Os range = 2.859(2)–2.916(2) Å). The $^{13}C\{^1H\}$ NMR spectrum of **1** indicates the carbonyl ligands are rigid at room temperature. Stirring **1** in CH_2Cl_2 for 2 days (ambient temperature) afforded $Os_4(\mu_3\text{-}\eta^2\text{-}C_2Ph_2)(CO)_{13}$ (**2**). The Os atoms in **2** also have an almost flat butterfly arrangement (Os—Os range = 2.7392(7)–2.8947(6) Å) with the alkyne ligand located over one of the Os_3 triangles. The ^{13}C NMR data for **2** are consistent with rapid rotation on the NMR timescale of the hinge $Os(CO)_3$ units at 21 °C, but slow rotation at –50 °C. Heating **2** at 40 °C gave $Os_4(\mu_4\text{-}\eta^2\text{-}C_2Ph_2)(CO)_{12}$ (**3**) after 2 days. Cluster **3** has the common butterfly arrangement of Os atoms with the C_2Ph_2 bound to all four metal atoms (Os—Os range = 2.7457(5)–2.8742(5) Å). The $^{13}C\{^1H\}$ NMR spectra of **3** at 21 and 90 °C indicate there is rapid CO exchange of the carbonyls of the two types of $Os(CO)_3$ units, but not between the units. The spectrum at –90 °C indicates one of the rotations (presumed to be that involving the carbonyls of the wingtip $Os(CO)_3$ units) is slowed on the NMR timescale. Compounds **1**–**3** form a unique series of clusters that have an alkyne ligand bound to two, three, and four metal atoms. Compound **1** is a model for a corner, compound **2** for a planar surface, and compound **3** a step site, in site-specific surface catalysts.

Key words: osmium cluster, diphenylacetylene, dimetallacyclobutene, carbonyl exchange, surface catalysis.

Résumé : On a préparé l'agrégat $Os_4(\mu\text{-}\eta^2\text{-}C_2Ph_2)(CO)_{14}$ (**1**) par réaction du $Os_4(CO)_{14}$ avec du C_2Ph_2, dans le CH_2Cl_2, à 25 °C; il était accompagné d'autres produits mineurs, dont les agrégats connus $Os_3(\mu_3\text{-}\eta^2\text{-}C_2Ph_2)(CO)_{10}$ et $Os_3(\mu\text{-}\eta^4\text{-}C_4Ph_4)(CO)_9$. La structure de **1** comporte un squelette C_2Os_4 approximativement plan avec un cycle dimétallacyclobutène (C—C = 1,32(4) Å) et une unité de Os_4 en forme de papillon applati (Os—Os = 2,859(2) à 2,916(2) Å). Les spectres RMN $^{13}C\{^1H\}$ du composé **1** indiquent que les ligands carbonyles sont rigides à la température ambiante. Par agitation pendant deux jours dans du CH_2Cl_2, à la température ambiante, le composé **1** conduit au $Os_4(\mu_3\text{-}\eta^2\text{-}C_2Ph_2)(CO)_{13}$ (**2**). Les atomes d'osmium dans le composé **2** adoptent aussi un arrangement en forme de papillon pratiquement plat (Os—Os = 2,7392(7) à 2,8947(6) Å) dans lequel le ligand alcyne se trouve au-dessus de l'un des triangles Os_3. Les données de la RMN du ^{13}C pour le composé **2** sont en accord avec une rotation rapide, à l'échelle de temps de la RMN et à 21 °C, des unités charnières $Os(CO)_3$; la rotation est toutefois lente à –50 °C. Par chauffage à 40 °C pendant deux jours, le composé **2** conduit à la formation du $Os_4(\mu_4\text{-}\eta^2\text{-}C_2Ph_2)(CO)_{12}$ (**3**). Dans l'agrégat **3**, les atomes d'osmium adoptent l'arrangement habituel en forme de papillon et le C_2Ph_2 est lié aux quatre atomes métalliques (Os—Os = 2,7457(5) à 2,8742(5) Å). Les spectres RMN $^{13}C\{^1H\}$ du composé **3** à 21 et 90 °C indiquent qu'il se produit un échange rapide de CO des carbonyles des deux types d'unités $Os(CO)_3$, mais qu'il n'y a pas d'échange entre les unités. Le spectre à –90 °C indique qu'une des rotations (probablement celle impliquant les carbonyles des unités $Os(CO)_3$ au bout des ailes) est ralentie à l'échelle de temps de la RMN. Les composés **1**, **2** et **3** forment une série unique d'agrégats comportant un ligand alcyne lié à deux, trois et quatre atomes métalliques. Les composés **1**, **2** et **3** sont respectivement un modèle pour un coin, pour une surface plane et pour un site étagé dans les catalyseurs de surface à site spécifique.

Mots clés : agrégat d'osmium, diphénylacétylène, dimétallacyclobutène, échange de carbonyle, catalyseur de surface.

[Traduit par la Rédaction]

Received 15 June 2005. Published on the NRC Research Press Web site at http://canjchem.nrc.ca on 28 February 2006.

This paper is dedicated to Professor Arthur J. Carty for his contributions to Canadian chemistry.

J.P. Canal and R.K. Pomeroy.[2] Department of Chemistry, Simon Fraser University, Burnaby, BC V5A 1S6, Canada.
M.C. Jennings. Department of Chemistry, University of Western Ontario, London, ON N6A 5B7, Canada.
G.P.A. Yap.[3] Department of Chemistry, University of Ottawa, Ottawa, ON K1N 6N5, Canada.

[1] This article is part of a Special Issue dedicated to Professor Arthur Carty.
[2] Corresponding author (e-mail: pomeroy@sfu.ca).
[3] Present address: Department of Chemistry and Biochemistry, University of Delaware, Newark, DE 19716, USA.

doi:10.1139/V05-239

Introduction

Alkynes form a plethora of complexes with group 8 metal carbonyls that have a remarkable structural diversity (1–3). For example, over 20 types of complexes have been isolated from the reaction of alkynes with $Fe_3(CO)_{12}$; they possess up to five metal atoms and three alkyne units (2, 4). Carty and co-workers (5, 6) have made notable contributions to the area, particularly alkyne derivatives of carbonyl clusters of ruthenium. The reaction of alkynes with $Os_3(CO)_{12}$ also provides novel products (3, 7–10).

In contrast to $Os_3(CO)_{12}$, the common carbonyl cluster of osmium (11), $Os_4(CO)_{14}$ readily undergoes substitution with two-electron donor ligands under mild conditions (12, 13). Here we describe the reaction of the tetraosmium cluster with diphenylacetylene to give the unique series $Os_4(\mu_x\text{-}\eta^2\text{-}C_2Ph_2)(CO)_{14-n}$ (n = 0, 1, 2; $x = n + 2$) in which a C_2Ph_2 molecule is successively bound to two, three, and four metal atoms. The dimetallacyclobutene cluster (i.e., the μ_2 compound) is of particular interest and is proposed as a model of corner sites of site-specific surface catalysts.

Experimental section

Unless otherwise stated, manipulations of starting materials and products were carried out under a nitrogen atmosphere with the use of standard Schlenk techniques. Hydrocarbon solvents were refluxed over potassium, distilled, and stored over molecular sieves before use. Dichloromethane was dried in a similar manner except that P_2O_5 was employed as the drying agent. The $Os_4(CO)_{14}$ was prepared by a literature procedure (13). The reactions were carried out in Carius tubes of volumes between 25–50 mL; each was fitted with a Teflon valve. NMR spectra were recorded on a Bruker AMX400 spectrometer at the appropriate operating frequencies for the ^1H and $^{13}C\{^1H\}$ NMR spectra. Samples of the complexes used for $^{13}C\{^1H\}$ NMR spectra were enriched to ~30% ^{13}CO. The samples were prepared from ^{13}CO-enriched $Os_4(CO)_{14}$, which in turn was prepared from ^{13}CO-enriched $Os_3(CO)_{12}$ (~40% ^{13}CO) (14).

Preparation of $Os_4(\mu\text{-}\eta^2\text{-}C_2Ph_2)(CO)_{14}$ (1)

To a solution of $Os_4(CO)_{14}$ (25 mg, 0.017 mmol) in CH_2Cl_2 (25 mL) at room temperature was added an excess of C_2Ph_2 (~20×) (C_2Ph_2 = diphenylacetylene). The solution was stirred for 105 min during which time the color of the solution changed from a red-brown to a deep red. The solvent was removed on the vacuum line and the remaining solid subjected to chromatography on a silica gel column (1.5 cm × 15 cm). Elution with hexanes removed the excess C_2Ph_2. Elution with hexanes–CH_2Cl_2 (90:10 by volume) gave several colored bands. The first (yellow) band was a trace amount of the known cluster $Os_3(\mu_3\text{-}\eta^2\text{-}C_2Ph_2)(CO)_{10}$. (In the preparations described below, the orange band of $Os_4(\mu_4\text{-}\eta^2\text{-}C_2Ph_2)(CO)_{12}$ (**3**) eluted next). This was followed by a red band that afforded $Os_4(\mu_3\text{-}\eta^2\text{-}C_2Ph_2)(CO)_{13}$ (**2**) in approximately 25% yield, then a purple band of another known cluster, $Os_3(\mu\text{-}\eta^4\text{-}C_4Ph_4)(CO)_9$, in <5% yield. Finally, a deep red band of the desired cluster **1** was obtained in about 70% yield. The analytical sample of **1** was obtained as air-stable, dark red (almost black) needles by recrystallization from CH_2Cl_2 and dried overnight under vacuum. IR (hexanes, cm^{-1}): ν(CO) 2126 (vw), 2080 (s), 2071 (m), 2065 (vw), 2044 (vs), 2025 (m), 1995 (m), 1909 (m). ^1H NMR (CD_2Cl_2) δ: 7.15–7.10 (m), 7.01–6.92 (m), 6.85–6.83 (dd). ^{13}C NMR (CD_2Cl_2, RT) δ: 192.13 (2C), 192.08 (2C), 185.6 (2C), 184.6 (1C), 176.6 (1C), 175.4 (2C), 172.5 (1C), 169.4 (1C), 169.3 (1C), 168.8 (1C), 128.1 (1C, Ph-*C*), 128.0 (2C, Ph-*C*), 126.6 (2C, Ph-*C*). MS (LI-MS) *m/z*: 1331.9 [M^+] (calcd. for M^+ = 1332 (100%), 1331 (81.5%)). Anal. calcd. for $C_{28}H_{10}O_{14}Os_4$: C 25.26, H 0.76; found: C 25.22, H 0.86.

$Os_3(\mu_3\text{-}\eta^2\text{-}C_2Ph_2)(CO)_{10}$

IR (hexanes, cm^{-1}): ν(CO) 2100 (m), 2066 (vs), 2047 (s), 2028 (s), 2011 (s), 1996 (m), 1982 (sh), 1965 (w) (in agreement with the literature values (7*a*)). ^{13}C NMR (CO region, RT) δ: 187.4 (2C), 186.8 (2C), 179.0 (1C), 174.5 (2C), 169.4 (1C), 168.0 (1C). MS (LI-MS) *m/z*: 1179.9 [M^+] (calcd. for M^+ = 1180 (100%), 1179 (86.1%)).

$Os_3(\mu\text{-}\eta^4\text{-}C_4Ph_4)(CO)_9$

IR (hexanes, cm^{-1}): ν(CO) 2113 (s), 2057 (vs), 2043 (vs), 2036 (sh), 2011 (vs), 1999 (m), 1990 (sh), 1974 (m), 1930 (m) (in agreement with the literature values (8*a*)). ^{13}C NMR (RT) δ: 175.7 (br s), 129.3 (2C, Ph-*C*), 128.1 (2C, Ph-*C*), 127.4 (1C, Ph-*C*). ^{13}C NMR (–60 °C) δ: 181.6 (~1C), 178.3 (~1C), 176.6 (~2C), 174.7 (~2C), 173.0 (~2C), 172.5 (~2C). MS (LI-MS) *m/z*: 1029.9 [M^+] (calcd. for M^+ = 1030 (100%), 1029 (83.3%)).

Preparation of $Os_4(\mu_3\text{-}\eta^2\text{-}C_2Ph_2)(CO)_{13}$ (2)

Cluster **2** was prepared in the same manner used to prepare **1**, except only a slight excess of C_2Ph_2 was used (~1:1.1) and the solution was allowed to stir at room temperature for 2 days. Again the solution changed from brown-red to a red over the reaction period. The desired product was isolated as described previously in about 60% yield. The analytical sample of **2** was obtained as air-stable, deep red crystals by recrystallization from CH_2Cl_2–hexanes. IR (hexanes, cm^{-1}): ν(CO) 2117 (m), 2078 (vs), 2046 (vs), 2040 (vs), 2012 (m), 1998 (m), 1987 (w), 1981 (w), 1963 (w), 1956 (w, sh). ^1H NMR (CD_2Cl_2) δ: 7.15–7.07 (m), 6.98–6.96 (m). ^{13}C NMR (CD_2Cl_2, RT) δ: 185.6 (1C, J_{CC} = 38.7 Hz), 182.6 (1C, J_{CC} = 37.2 Hz), 180.5 (1C), 176.5 (6C), 173.2 (1C), 169.3 (1C), 130 (2C, Ph-*C*), 127.8 (2C, Ph-*C*), 127.6 (1C, Ph-*C*). ^{13}C NMR (CD_2Cl_2, –50 °C) δ: 185.6 (1C), 181.8 (1C), 180.2 (1C), 177.6 (2C), 175.8 (2C), 175.2 (2C), 172.8 (2C), 169.0 (2C). MS (LI-MS) *m/z*: 1303.6 [M^+] (calcd. for M^+ = 1304 (100%), 1303 (87.4%)). Anal. calcd. for $C_{27}H_{10}O_{13}Os_4$: C 24.85, H 0.77; found: C 25.01, H 0.98.

Preparation of $Os_4(\mu_4\text{-}\eta^2\text{-}C_2Ph_2)(CO)_{12}$ (3)

The same reaction conditions used to produce **2** were employed except the reaction mixture was heated to 40 °C for 2 days. Over the time period the solution went from brown-red through dark red to orange-red as the initially produced **1** went to **2** and then **3**. The desired product in ~90% yield was isolated in the normal manner. (In an alternate procedure, **3** was isolated in 90% yield when either **1** or **2** was allowed to stir at room temperature in hexanes for 18 days). The analytical sample of **3** was obtained as air-stable, sparkling red-orange crystals by recrystallization from CH_2Cl_2. IR (hexanes, cm^{-1}): ν(CO) 2098 (m), 2071 (vs), 2046 (vs), 2041 (vs), 2019 (s), 2000 (s), 1982 (w), 1971 (m). ^1H NMR

Table 1. Details of the crystal structure determinations of **1**·CH_2Cl_2, **2**, and **3**.

Structure name	**1**·CH_2Cl_2	**2**	**3**
Compound	$C_{28}H_{10}O_{14}Os_4$	$C_{27}H_{10}O_{13}Os_4$	$C_{26}H_{10}O_{12}Os_4$
Formula weight	1416.09	1 303.15	1275.14
Crystal system	Monoclinic	Triclinic	Monoclinic
T (°C)	–123	–70	–70
Space group	$P2_1/n$	P-1	$P2_1/c$
a (Å)	8.8718(6)	12.492(1)	9.634(1)
b (Å)	25.138(2)	15.179(1)	16.743(2)
c (Å)	14.814(1)	15.923(1)	17.127(2)
α (°)	90	78.215(1)	90
β (°)	97.564(2)	85.257(1)	90.390(2)
γ (°)	90	84.797(2)	90
Cell volume (Å^3), Z	3275.0(4), 4	2 937.0(4), 4	2762.7(5), 4
$D_{\mathrm{calcd.}}$ (Mg m^{-3})	2.872	2.947	3.066
Abs. coeff (mm^{-1})	15.701	17.315	18.402
Unique data ($I > 2\sigma$)	3053	12 503	6466
R^a	0.0622	0.0539	0.0424
$R_w{}^b$	0.1063	0.1584	0.1101

[a] $R = \Sigma|(|F_o| - |F_c|)|/\Sigma|F_o|$.

[b] $R_w = [\Sigma(w(|F_o| - |F_c|)^2)/\Sigma(wF_o{}^2)]^{1/2}$, $w = [\sigma^2(F_o)^2 + kF_o{}^2]^{-1}$.

(CD_2Cl_2) δ: 7.21–7.17 (m), 7.14–7.10 (m). ^{13}C NMR (toluene-d_8, 90 °C) δ: 180.4 (s, 6C), 175.5 (s, 6C). ^{13}C NMR (CD_2Cl_2, RT) δ: 180.5 (6C, J_{OsC} (^{187}Os) = 106.9 Hz), 175.5 (6C, J_{OsC} = 117.5 Hz), 132.5 (2C, Ph-*C*), 129.3 (1C, Ph-*C*), 127.2 (2C, Ph-*C*). ^{13}C NMR (CD_2Cl_2, –90 °C) δ: 180.5 (s, 6C), 175.5 (w/broad, 6C). MS (LI-MS) *m/z*: 1275.6 [M$^+$] (calcd. for M$^+$ = 1276 (100%), 1275 (87.4%)). Anal. calcd. for $C_{26}H_{10}O_{12}Os_4$: C 24.45, H 0.78; found: C 24.65, H 0.88.

X-ray structural determinations

The structure of **1** was determined at the University of Western Ontario, London, Ontario. Crystals of **1**·CH_2Cl_2 were grown from a concentrated dichloromethane solution. A red-orange, flat needle was cut and mounted on a glass fiber. Data were collected at low temperature (–123 °C) on a Nonius Kappa-CCD diffractometer. The unit cell parameters were calculated and refined from the full data set. Crystal cell refinement and data reduction were carried out with the program DENZO and the data were scaled with the program SCALEPACK. The crystal data and refinement parameters for **1**·CH_2Cl_2 are listed in Table 1. The reflection data and systematic absences were consistent with a monoclinic space group, *P*2(1)/*n*. The SHELXTL-NT V6.1 (G. Sheldrick) suite of programs was used to solve the structure by direct methods. Subsequent difference Fourier syntheses allowed the remaining atoms to be located. The osmium atoms were refined with anisotropic thermal parameters. The remaining atoms were refined isotropically. The hydrogen atom positions were calculated geometrically and were included as riding on their respective carbon atoms. The solvent molecule was refined fully anisotropically and the C—Cl distances were fixed at 1.72 Å. Due to the poor quality of the crystal, good data was only obtained to 20° on θ. The largest residue electron density peak (2.02 e/Å^3) was associated with one of the osmium–osmium bonds. Full-matrix least-squares refinement on F^2 gave R_1 = 6.22 for 2σ data and wR_2 = 12.64 for all data (GOF = 1.134).

The structures of **2** and **3** were determined at the University of Ottawa, Ottawa, Ontario. Suitable crystals were selected, mounted with Paratone oil on glass fibres, and flash-cooled to the data collection temperature of –70 °C. Unit-cell parameters were obtained from 60 data frames, 0.3° θ, from three different sections of the Ewald sphere. No symmetry higher than triclinic was observed in the diffraction data for **2** and solution in the centrosymmetric space group option, *P*-1, yielded chemically reasonable and computationally stable results of refinement. The unit-cell parameters and systematic absences in the diffraction data of **3** were uniquely consistent with the space group $P2_1/c$. The data sets were corrected for absorption with the Bruker SADABS program based on redundant data. Two symmetry-unique, but chemically equivalent molecules were located in the asymmetric unit of **2**. Features remaining in the final difference Fourier electron density map of **2** were located <0.9 Å from osmium atoms and were ignored as noise artifacts. All non-hydrogen atoms were refined with anisotropic displacement parameters. All hydrogen atoms were treated as idealized contributions. Structure factors are contained in the SHELXTL 6.12 program library. A summary of the data collection and refinement for each structure are given in Table 1.[4]

---

[4] Supplementary data for this article are available on the journal Web site (http://canjchem.nrc.ca) or may be purchased from the Depository of Unpublished Data, Document Delivery, CISTI, National Research Council Canada, Ottawa, ON K1A 0R6, Canada. DUD 4089. For more information on obtaining material refer to http://cisti-icist.nrc-cnrc.gc.ca/irm/unpub_e.shtml. CCDC 279768–279770 contain the crystallographic data for this manuscript. These data can be obtained, free of charge, via http://www.ccdc.cam.ac.uk/conts/retrieving.html (Or from the Cambridge Crystallographic Data Centre, 12 Union Road, Cambridge CB2 1EZ, UK; fax +44 1223 336033; or deposit@ccdc.cam.ac.uk).

Fig. 1. Molecular structure of $Os_4(\mu\text{-}\eta^2\text{-}C_2Ph_2)(CO)_{14}$ (**1**).

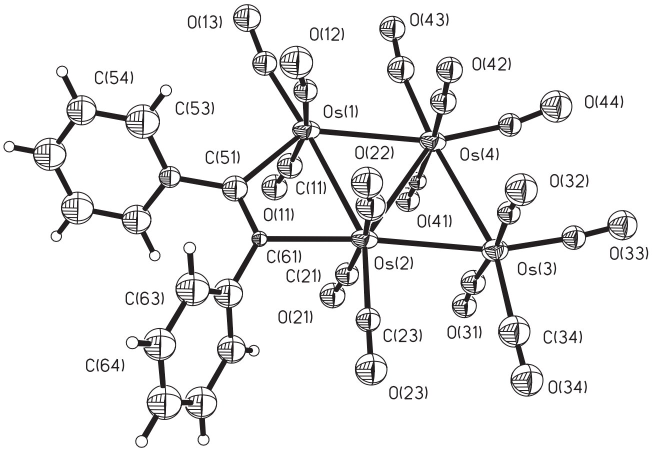

Results and discussion

$Os_4(\mu\text{-}\eta^2\text{-}C_2Ph_2)(CO)_{14}$ (1)

Compound **1** was isolated as dark red needles in about 70% yield from the reaction of $Os_4(CO)_{14}$ in CH_2Cl_2 with an excess of C_2Ph_2 at room temperature (eq. [1]).

[1] $$Os_4(CO)_{14} + C_2Ph_2 \xrightarrow[CH_2Cl_2]{25\ ^\circ C} Os_4(\mu\text{-}\eta^2\text{-}C_2Ph_2)(CO)_{14}\ (\mathbf{1}) + \text{other products}$$

(By comparison, the reaction of $Os_3(CO)_{12}$ with C_2Ph_2 requires temperatures of 160 °C or above to proceed at a measurable rate (9)). An excess of the acetylene ensured that **1** formed quickly as it slowly loses CO to give $Os_4(\mu_3\text{-}\eta^2\text{-}C_2Ph_2)(CO)_{13}$ (**2**). Besides **2**, other products isolated from the reaction shown in eq. [1] were the known clusters $Os_3(\mu_3\text{-}\eta^2\text{-}C_2Ph_2)(CO)_{10}$ (7) and $Os_3(\mu\text{-}\eta^4\text{-}C_4Ph_4)(CO)_9$ (8, 9). The stereochemical nonrigidity of the former cluster has been investigated by variable-temperature $^{13}C\{^1H\}$ NMR spectroscopy (15) and found similar to the nonrigidity exhibited by $Os_3(\mu_3\text{-}\eta^2\text{-}C_2R_2)(CO)_{10}$ (R = Me, Et) (10). All products are brightly colored and were readily separated by column chromatography. The derivatives appeared air stable, although crystals of **1** deteriorated on standing. This can be attributed to either loss of CO (to give **2**) or loss of the CH_2Cl_2 of crystallization. (Crystals of **1** suitable for the structural determination were obtained only after some difficulty).

Compound **1** was characterized by C/H/N analysis, IR, mass (parent ion), ^1H and ^{13}C NMR spectroscopy, and X-ray crystallography. The structure of **1** (as the CH_2Cl_2 solvate) reveals an approximately planar Os_4C_2 unit (Fig. 1); selected bond lengths and angles for **1** are given in Table 2. The Os_4 unit adopts a flat butterfly arrangement with five Os—Os bonds that range in length from 2.859(2) to 2.916(2) Å. These lengths are typical for open Os carbonyl clusters and may be compared with the average Os—Os bond distance in $Os_3(CO)_{12}$ of 2.877 Å (16). If it is assumed that the Os—Os bonds are single nondative covalent bonds, then Os(1) has a 17 electron count and Os(4) a 19 electron count. The Os(1)—Os(4) can therefore be regarded as a dative metal–metal bond with the Os(4) atom donating two electrons to Os(1) (17). Interestingly, it is the shortest Os—Os bond in **1**. We have reported numerous complexes that contain unsupported Os—M (M = transition metal) dative bonds (18).

Table 2. Selected bond lengths (angstroms) and angles (degrees) for **1**.

Bond lengths (Å)	
Os(1)—Os(2)	2.866(2)
Os(1)—Os(4)	2.859(2)
Os(2)—Os(3)	2.880(2)
Os(2)—Os(4)	2.916(2)
Os(3)—Os(4)	2.907(2)
C(51)—C(61)	1.32(4)
Os(1)—C(51)	2.13(3)
Os(2)—C(61)	2.28(3)
Os—C(CO) range	1.84(3)–1.96(3)
Bond angles (°)	
Os(1)-Os(2)-Os(3)	119.44(6)
Os(1)-Os(2)-Os(4)	59.25(5)
Os(1)-Os(4)-Os(2)	59.51(4)
Os(1)-Os(4)-Os(3)	118.77(6)
Os(2)-Os(1)-Os(4)	61.25(5)
Os(2)-Os(3)-Os(4)	60.52(4)
Os(2)-Os(4)-Os(3)	59.28(4)
Os(3)-Os(2)-Os(4)	60.20(4)
Os(1)-Os(2)-C(61)	65.5(6)
Os(2)-Os(1)-C(51)	73.5(8)
Os(1)-C(51)-C(52)	126(2)
Os(1)-C(51)-C(61)	108(2)
Os(2)-C(61)-C(51)	113(2)
Os(2)-C(61)-C(62)	119(2)
C(52)-C(51)-C(61)	126(3)
C(62)-C(61)-C(51)	128(3)

Cluster **1** possesses a dimetallacyclobutene ring (i.e., Os(1)-Os(2)-C(61)-C(51)). The geometry about each C atom of the unit is approximately trigonal planar, although the internal Os-C-C angles (108(2)° and 113(2)°) are somewhat compressed from the ideal value of 120°. The C—C bond length of 1.32(4) Å is consistent with an uncoordinated C=C double bond. The Os—C bond lengths to the alkyne are 2.13(3) (to Os(1)) and 2.28(3) Å (to Os(2)). Because of the somewhat poor quality of the data, it is not clear that the difference is significant, or a genuine electronic effect: Os(1) is six-coordinate, whereas Os(2) is seven-coordinate. The lengths may be compared with the Os—C lengths to the carbonyl ligands in **1** that are in the range 1.84(4) to 1.95(3) Å.

Dimetallacyclobutene compounds are comparatively rare and a search of the literature (SciFinder Scholar) of this term yielded only 11 publications containing compounds with this bonding motif (1, 19–23). Some recent examples are $Ir_2(\mu\text{-}\eta^2\text{-}C_2R_2)(\eta^5\text{-}C_9H_7)_2(CO)_2$ (R = Ph, Tol) (20) and $Re_2Cp^*_2(\mu\text{-}\eta^2\text{-}C_2(CO_2CH_3)_2(CO)_4$ (21). Only one compound, $Ir_4[(\mu\text{-}\eta^2\text{-}C_2(MeCO_2)_2]_2[(\mu_4\text{-}\eta^2\text{-}C_2(MeCO_2)_2]_2(CO)_8$, contains more than two metal atoms, that is, it is a cluster compound (22). The bond lengths and angles in **1** are comparable to those found in $Os_2[\mu\text{-}\eta^2\text{-}C_2(CO_2Me)_2](CO)_8$ (C—C bond = 1.33(1) Å; both Os—C bonds = 2.138(5) Å; Os-C-C angle = 111.2(2)°) (23). The C—C bond length in **1** may be also be compared with the corresponding length (1.53(3) Å) in the saturated Os-C-C-Os unit in $Os_2(\mu\text{-}\eta^2\text{-}C_2H_4)(CO)_8$ (24).

Fig. 2. The $^{13}C\{^1H\}$ NMR spectrum (CO region) of **1** (^{13}CO enriched) in CH_2Cl_2–CD_2Cl_2 (4:1) at 21 °C.

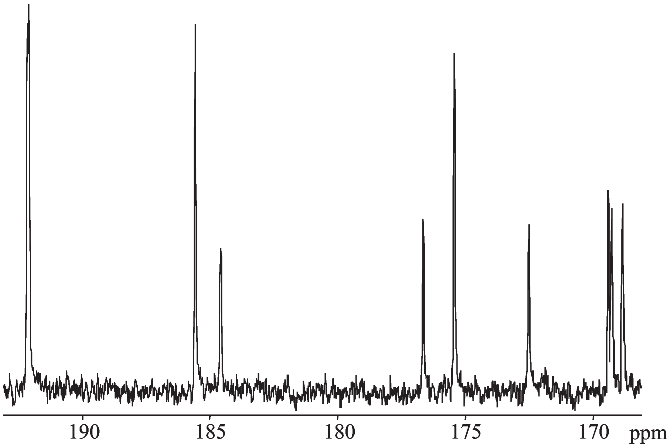

The $^{13}C\{^1H\}$ NMR spectrum of **1** (^{13}CO enriched) in CD_2Cl_2–CH_2Cl_2 at ambient temperature exhibits four signals of intensity 2 and six signals of intensity 1 in the carbonyl region (Fig. 2). This observation is consistent with the view that **1** has the same structure in solution as that in the solid state, and the carbonyls are rigid on the NMR timescale at this temperature. Typically, resonances due to axial carbonyl ligands come to low field of those due to equatorial carbonyls (14, 25). As can be seen from Fig. 2, one signal of intensity 2 is shifted to higher field and one signal of intensity 1 to lower field. These atypical signals are tentatively assigned to the carbonyls attached to Os(1) because of the unusual bonding at this atom.

$Os_4(\mu_3\text{-}\eta^2\text{-}C_2Ph_2)(CO)_{13}$ (2)

When **1** was stirred in CH_2Cl_2 at room temperature for 2 days cluster **2** was produced in good yield (eq. [2]). The product was isolated after chromatography as red crystals that were characterized by C/H/N analysis, IR, mass (parent ion), ^1H and ^{13}C NMR spectroscopy, and X-ray crystallography.

$$[2] \quad Os_4(\mu\text{-}\eta^2\text{-}C_2Ph_2)(CO)_{14} \xrightarrow[\text{2 days}]{25\ °C} Os_4(\mu_3\text{-}\eta^2\text{-}C_2Ph_2)(CO)_{13}\ (\mathbf{2}) + CO$$

The structure of **2** has two independent molecules in the unit cell that differ in the orientation of the phenyl rings, but are otherwise identical. A view of one of the molecules (molecule **2A**) is given in Fig. 3; selected bond lengths and angles for each molecule are collected in Table 3. The structure of **2** consists of an almost flat butterfly arrangement, as found in **1**, with the alkyne spanning one of the Os_3 triangles. The peripheral Os—Os lengths associated with the alkyne in each molecule (range = 2.7392(7)–2.7740(7) Å) are significantly shorter than the peripheral Os—Os lengths that involve Os atoms not directly bound to the C_2Ph_2 (range 2.8665(6)–2.8947(6) Å). The shorter Os—Os bonds can be attributed to the bonding requirements of the bridging C_2Ph_2 ligand. The unbridged Os—Os bonds are typical for open Os clusters. The hinge Os—Os bonds in each molecule are of intermediate length (2.8204(6) and 2.8007(7) Å).

Fig. 3. Molecular structure of $Os_4(\mu_3\text{-}\eta^2\text{-}C_2Ph_2)(CO)_{13}$ (**2**).

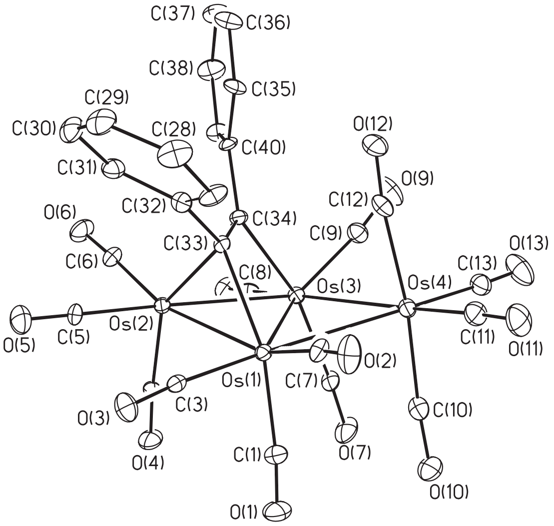

The 18-electron rule requires that the alkyne fragment donates two electrons to the wingtip Os atom (e.g., Os(2) in molecule **2A**) and one electron to each hinge Os atom (e.g., Os(1) and Os(3) in **2A**). The Os—C(alkyne) lengths that involve the wingtip Os atoms (e.g., Os(2) and Os(6)) are in the range 2.27(1)–2.29(1) Å and are somewhat longer than the other Os—C(alkyne) lengths in **2** (range 2.15(1)–2.18(1) Å). The bonding may be viewed as a dimetallacyclobutene unit with the C=C double bond acting as a typical alkene ligand toward the wingtip Os atom. The length of the C—C bond (1.42 Å) of the alkyne unit suggests a formal bond order less than two, as observed in similar compounds (7, 10, 26, 27). The bonding of the alkyne to the Os_3 triangle in **2** is similar to that in compounds such as $Os_3(\mu_3\text{-}\eta^2\text{-}C_2R_2)(CO)_{10}$ (R = Et (10), R = Ph (7)), $Os_5(\mu_3\text{-}\eta^2\text{-}C_2H_2)(CO)_{17}$ (26), and $Os_7(\mu_3\text{-}\eta^2\text{-}C_2Me_2)(CO)_{19}$ (27).

The $^{13}C\{^1H\}$ NMR spectra in the carbonyl region of **2** (^{13}CO enriched) in CD_2Cl_2–CH_2Cl_2 at –50 and 21 °C are shown in Fig. 4. The lower temperature spectrum exhibits eight signals in an approximate 1:1:1:2:2:2:2:2 (low to high field). This is consistent with the view that **2** has the same structure in solution as in the crystalline state, and that the carbonyls are rigid on the NMR timescale at –50 °C. The two signals at lowest field (i.e., at δ 185.6 and 181.8) exhibit satellites and are therefore readily assigned to the C atoms of the two chemically different axial CO ligands on the unbridged wingtip Os atom (i.e., the C atoms C(23) and C(25) in Fig. 3). This is because only these peaks would be expected to exhibit observable ^{13}C–^{13}C coupling owing to the mutual trans arrangement of these carbonyls. (Recall the complex was ^{13}CO enriched.) The remaining signal of intensity 1 (at δ 180.2) is attributed to the axial carbonyl atom on the bridged wingtip Os atom (i.e., C(17)). The signal at δ 177.6 is assigned to the two C atoms of the axial carbonyls on the hinge Os atoms (i.e., C(14) and C(20)). As stated previously, ^{13}C NMR resonances due to C atoms of axial carbonyls usually appear to lower field than the corresponding signals of equatorial carbonyls. The resonances at δ 175.8 and 175.2 are assigned to the C atoms of the equatorial carbonyls on the hinge Os atoms on the basis of their exchange behavior described in the following paragraph. The remain-

Table 3. Selected bond lengths (angstroms) and angles (degrees) for **2**.

Molecule **A**		Molecule **B**	
Bond lengths (Å)			
Os(1)—Os(2)	2.7586(6)	Os(5)—Os(6)	2.7392(7)
Os(1)—Os(3)	2.8204(6)	Os(5)—Os(7)	2.8007(7)
Os(1)—Os(4)	2.8665(6)	Os(5)—Os(8)	2.8871(7)
Os(2)—Os(3)	2.7454(6)	Os(6)—Os(7)	2.7740(7)
Os(3)—Os(4)	2.8947(6)	Os(7)—Os(8)	2.8939(7)
C(33)—C(34)	1.42(2)	C(47)—C(48)	1.42(2)
Os(5)—C(47)	2.17(1)	Os(5)—C(47)	2.17(1)
Os(6)—C(47)	2.29(1)	Os(6)—C(47)	2.29(1)
Os(6)—C(48)	2.29(1)	Os(6)—C(48)	2.29(1)
Os(7)—C(48)	2.16(1)	Os(7)—C(48)	2.16(1)
Os—C(CO) range	1.88(1)–1.99(1)		
Bond angles (°)			
Os(1)-Os(2)-Os(3)	61.65(2)	Os(5)-Os(6)-Os(7)	61.06(2)
Os(1)-Os(3)-Os(2)	59.41(2)	Os(5)-Os(7)-Os(6)	58.86(2)
Os(1)-Os(3)-Os(4)	60.19(2)	Os(5)-Os(7)-Os(8)	60.90(2)
Os(1)-Os(4)-Os(3)	58.62(2)	Os(5)-Os(8)-Os(7)	57.96(2)
Os(2)-Os(1)-Os(3)	58.94(2)	Os(6)-Os(5)-Os(7)	60.08(2)
Os(2)-Os(1)-Os(4)	118.26(2)	Os(6)-Os(5)-Os(8)	118.54(2)
Os(2)-Os(3)-Os(4)	117.74(2)	Os(6)-Os(7)-Os(8)	117.15(2)
Os(3)-Os(1)-Os(4)	61.19(2)	Os(7)-Os(5)-Os(8)	61.14(2)
Os(1)-Os(2)-C(33)	49.2(3)		
Os(1)-C(33)-Os(2)	76.8(3)		
Os(2)-Os(1)-C(33)	54.0(3)		
Os(2)-Os(3)-C(34)	53.5(3)		
Os(2)-C(34)-Os(3)	76.1(4)		
Os(3)-Os(2)-C(33)	70.6(3)		
Os(1)-Os(3)-C(34)	71.1(3)		
Os(3)-Os(1)-C(33)	71.0(3)		
Os(1)-C(33)-C(34)	110.4(8)		
Os(3)-C(34)-C(33)	107.5(8)		
Os(2)-C(33)-C(34)	71.2(6)		
Os(2)-C(34)-C(33)	72.6(6)		
C(33)-Os(2)-C(34)	36.1(4)		
Os(1)-C(33)-C(32)	124.2(8)		
Os(2)-C(33)-C(32)	120.7(8)		
Os(2)-C(34)-C(40)	125.2(8)		
Os(3)-C(34)-C(40)	125.4(8)		
C(32)-C(33)-C(34)	125(1)		
C(40)-C(34)-C(33)	126(1)		

Note: Two independent molecules in the unit cell.

ing resonances at δ 172.8 and 169.0 are attributed to the C atoms of the equatorial carbonyls on the wingtip Os atoms. The latter signal is attributed to the carbonyls of the $Os(CO)_4$ grouping since it remains sharp in the spectrum at ambient temperature (see the following paragraph).

In the spectrum at 21 °C, three of the resonances have coalesced to a broad singlet (Fig. 4), indicative of exchange between the carbonyls that give rise to the signals in the spectrum at lower temperature. This is attributed to carbonyl exchange of the hinge $Os(CO)_3$ groupings. Rotation of $Os(CO)_3$ units in condensed Os carbonyl clusters is common. Examples are $Os_6(CO)_{17}(L)$ (L = CO, PPh_3) (28, 29) and $Os_7(CO)_{21}$ (30). The hinge Os atoms are seven-coordinate, whereas the wingtip Os atoms are nominally six-coordinate (if the bond to the C_2Ph_2 is a conventional metal–alkene bond). It is well-known that mononuclear six-coordinate complexes are usually rigid, whereas the corresponding seven-coordinate complexes are invariably nonrigid in solution.

Although the reason for the difference in activation barriers to exchange may be based upon electronic considerations, it can be rationalized by using simple steric arguments. We have shown that the ground-state and transition-state energies are both important in determining a barrier to rotation of the arene ring in (η^6-arene)$Fe(CO)_2(SiCl_3)$ complexes (31). In six-coordinate complexes, the trigonal prismatic transition state for $M(CO)_3$ rotation has three eclipsing interactions as depicted in Scheme 1. Also of importance is that in the ground state all the substituents are perfectly staggered with their nearest neighbors and hence it is at a low

Fig. 4. The $^{13}C\{^1H\}$ NMR spectrum (CO region) of **2** (^{13}CO enriched) in CH_2Cl_2–CD_2Cl_2 (4:1) at 21 and –50 °C.

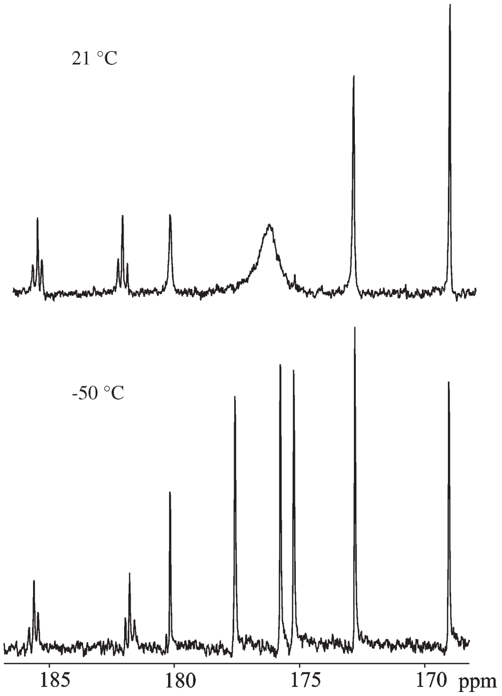

energy. In a seven-coordinate complex, the transition state to rotation of a trigonal unit only has two close eclipsing interactions in the transition state and therefore might be expected to be at a lower energy than the transition-state energy in the six-coordinate case (Scheme 1). What may not be realized is that in the seven-coordinate configuration the ground state is destabilized relative to the six-coordinate configuration because in the higher coordination case there are still close interactions in the lowest energy conformation.

In the spectrum at 21 °C, the signals attributed to the wingtip $Os(CO)_3$ group have broadened relative to the signals owing to the wingtip $Os(CO)_4$ unit. This probably indicates the onset of rotation on the NMR timescale of this $Os(CO)_3$ group and is relevant to the discussion on the rotation of the $Os(CO)_3$ units in **3** discussed in the following. The NMR spectrum of **2** at higher temperatures was not investigated because of its ready decarbonylation to **3**.

$Os_4(\mu_4\text{-}\eta^2\text{-}C_2Ph_2)(CO)_{12}$ (3)

When the reaction shown in eq. [2] was carried out at 40 °C, $Os_4(\mu_4\text{-}\eta^2\text{-}C_2Ph_2)(CO)_{12}$ (**3**) was isolated in ~90% yield (eq. [3]). The cluster, as bright orange-red, air-stable crystals, was characterized by C/H/N analysis, IR, mass (parent ion), ^1H and ^{13}C NMR spectroscopy, and by X-ray crystallography. Compound **3** has remarkable thermal stability. Overnight pyrolysis of **3** in C_6F_6 under vacuum at 230 °C had little effect on the cluster; decomposition (in part to $Os_3(CO)_{12}$) only commenced at 250 °C. Even after 4 days at 250 °C **3** had not completely decomposed.

$$[3] \quad Os_4(\mu_3\text{-}\eta^2\text{-}C_2Ph_2)(CO)_{13} \xrightarrow[\text{2 days}]{40\ ^\circ C} Os_4(\mu_4\text{-}\eta^2\text{-}C_2Ph_2)(CO)_{12} + (\mathbf{3})\ CO$$

Scheme 1.

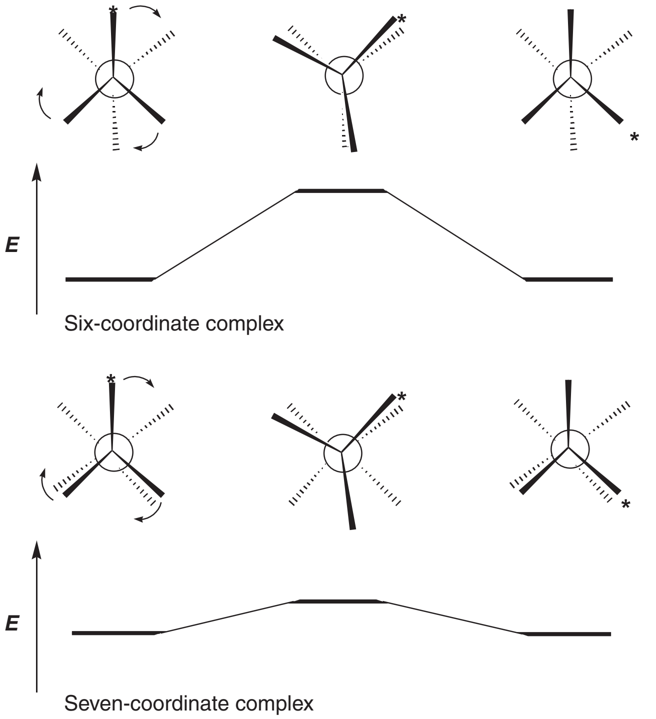

Although the Ru analogue of **3** has been known since 1977 (32), the Os compound has not been previously reported (SciFinder Scholar). A view of the structure of **3** is shown in Fig. 5. The structure is typical of clusters of the formula, $M_4(\mu_4\text{-}\eta^2\text{-}C_2RR')(CO)_{12}$ (M = Fe, Ru, Os) (1–3, 6, 32–34). These clusters may be viewed as electron-deficient butterfly clusters with 60 cluster valence electrons, or as *closo* octahedral clusters with seven skeletal electron pairs according to PSEPT (6). In **3** the peripheral Os—Os bonds range in length from 2.7457(5) to 2.7652(5) Å (Table 4), lengths that are typical of Os—Os lengths in condensed Os clusters. The hinge Os(1)—Os(3) bond is longer at 2.8742(5) Å. The four Os—C lengths of the alkyne unit to the wingtip Os atoms (Os(2) and Os(4)) are slightly longer (2.251(7)–2.274(8) Å) than the Os—C lengths to the hinge Os atoms (2.179(8), 2.201(8) Å). The pattern of the Os—Os and Os—C lengths closely match those previously found in $Ru_4(\mu_4\text{-}\eta^2\text{-}C_2Ph_2)(CO)_{12}$ (32) and $Os_4(\mu_4\text{-}\eta^2\text{-}C_2H_2)(CO)_{12}$ (34). The C—C bond length (1.49(1) Å) of the alkyne ligand in **3** is the longest of the three alkyne C—C lengths determined in this study and is close to that of a C—C single bond length.

Carbon-13 NMR spectra in the carbonyl region of **3** (^{13}CO enriched) at different temperatures are shown in Fig. 6. If the carbonyl groups were rigid, each chemically distinct $Os(CO)_3$ (i.e., wingtip and hinge moieties) unit would give rise to a 2:1 or 1:1:1 pattern of signals in the NMR spectrum (32). It is apparent that at 21 and 90 °C there is rapid rotation of the two different types of $Os(CO)_3$ groupings in **3**, but that migration of CO ligands between the wingtip and hinge Os atoms does not occur on the NMR timescale. This is also observed in clusters such as $Os_6(CO)_{18}$ (28).

In the spectrum at –90 °C, one of the signals has collapsed almost to the baseline, indicative of slowed exchange

Fig. 5. Molecular structure of $Os_4(\mu_4-\eta^2-C_2Ph_2)(CO)_{12}$ (**3**).

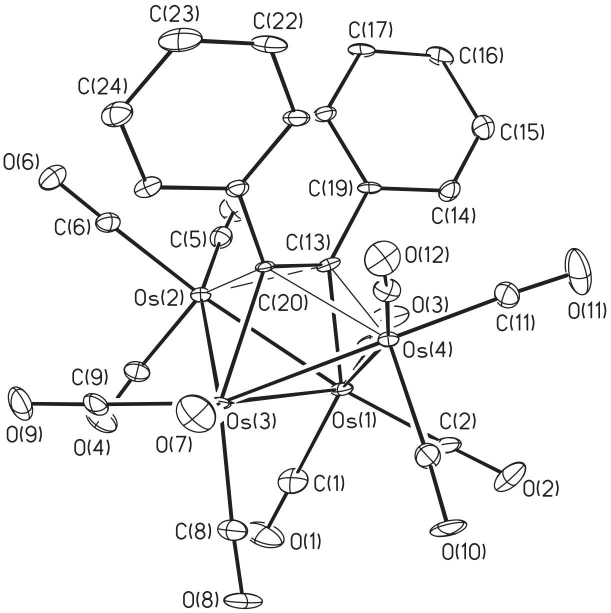

Table 4. Selected bond lengths (angstroms) and angles (degrees) for **3**.

Bond lengths (Å)	
Os(1)—Os(2)	2.7515(5)
Os(1)—Os(3)	2.7592(5)
Os(1)—Os(4)	2.8742(5)
Os(2)—Os(3)	2.7652(5)
Os(3)—Os(4)	2.7457(5)
Os—C(CO) range	1.908(9)–1.95(1)
C(13)—C(20)	1.49(1)
Os(1)—C(13)	2.179(8)
Os(2)—C(13)	2.274(8)
Os(2)—C(20)	2.265(7)
Os(3)—C(20)	2.201(7)
Os(4)—C(13)	2.255(8)
Os(4)—C(20)	2.251(7)
Bond angles (°)	
Os(1)-Os(2)-Os(3)	62.80(1)
Os(1)-Os(3)-Os(2)	58.37(1)
Os(2)-Os(1)-Os(3)	58.83(1)
Os(1)-Os(3)-Os(4)	58.76(1)
Os(1)-Os(4)-Os(3)	62.95(1)
Os(3)-Os(1)-Os(4)	58.30(1)
Os(1)-Os(2)-C(13)	50.3(2)
Os(1)-C(13)-Os(2)	76.3(3)
Os(2)-Os(1)-C(13)	53.4(2)
Os(1)-Os(4)-C(13)	52.7(2)
Os(4)-Os(1)-C(13)	52.7(2)
Os(1)-C(13)-Os(4)	76.9(2)
Os(2)-Os(3)-C(20)	52.8(2)
Os(3)-Os(2)-C(20)	50.7(2)
Os(2)-C(20)-Os(3)	76.5(2)
Os(3)-Os(4)-C(20)	51.1(2)
Os(4)-Os(3)-C(20)	52.7(2)
Os(3)-C(20)-Os(4)	76.2(2)
Os(2)-C(13)-C(20)	70.5(4)
Os(2)-C(20)-C(13)	71.1(4)
C(13)-Os(2)-C(20)	38.4(3)
Os(4)-C(13)-C(20)	70.5(4)
Os(4)-C(20)-C(13)	70.8(4)
C(13)-Os(4)-C(20)	38.7(3)
Os(2)-Os(1)-Os(4)	91.67(1)
Os(1)-C(13)-C(19)	125.1(6)
Os(3)-C(20)-C(26)	125.6(6)
C(19)-C(13)-C(20)	126.3(7)
C(13)-C(20)-C(26)	126.0(7)

of one of the pairs of $Os(CO)_3$ units. This was also observed in the variable-temperature ^{13}C NMR spectra of $Ru_4(\mu_4-\eta^2-C_2Ph_2)(CO)_{12}$ (32). Given the fluxional behavior of the $Os(CO)_3$ units in **2**, it is probable that the carbonyls that are still undergoing rapid exchange in **3** are those of the hinge $Os(CO)_3$ units.

Clusters 1–3 as models for surface catalysts

As mentioned in the Introduction, **1**–**3** form a unique series of clusters in which an alkyne ligand is successively bound to two, three, and four metal atoms. Indeed, any series of structurally characterized clusters that involves the stepwise loss of two carbonyls are rare. One such series, however, is $Co_4(CO)_x(PNR_2)_2$ (x = 8, 9, or 10) recently reported by Carty and co-workers (35).

Muetterties et al. (36, 37) first pointed out that the structures of molecular clusters may provide insight to the understanding of surface catalysis. Despite its importance and intense study, the precise nature of the active sites in surface catalysts is still unknown (38–42). Recent investigations by physical techniques indicate that the catalytic properties of small particles depend on their size and imperfections (43, 44). For example, a recent study by Wei and Iglesia (44) of CH_4 reactions on Ru-based catalysts concluded that edge and corner atoms, with fewer Ru neighbors than those on terraces, were primarily responsible for C-H activation. We believe that compounds **1**–**3** may provide insight to the understanding of these active sites. In Table 5 the C—C and Os—C bond lengths for **1**–**3** are collected together for ready comparison. Scheme 2 summarizes the preparation of the clusters from $Os_4(CO)_{14}$.

Cluster **1** is a model for an alkyne bound to a corner site of a metal surface; compound **2** is a model for an alkyne bound to a planar metal surface; whereas **3**, with its butterfly arrangement of metal atoms, is a model for an alkyne bound to a step site of a metal surface. Although step sites have been proposed as the active sites of surface catalysts (6, 37, 38), the data in Table 5 indicates that the alkyne is tightly bound to the Os atoms in **3** and as such would be unreactive. Consider, for example, the thermal stability of **3**. The alkyne also appears to be tightly bound to the Os_4 unit in **2**, although less so than in **3**

On the other hand, the C_2Ph_2 molecule in **1** is bound to the Os_4 nucleus via two σ bonds, one of which is long (Table 5). It might be expected that there would also be considerable ring strain in the diosmacyclobutene unit. Furthermore, because of the proximity of the osmium atoms the frontier orbitals about the C atoms in the bound C_2Ph_2 will

Table 5. The C—C and Os—C bond lengths of the alkyne-Os unit in **1**–**3**.

Compound	C—C bond lengths (Å)	Os—C bond lengths (Å) (σ)	Os—C bond lengths (Å) (π)
1	1.32(4)	2.13(3), 2.28(3)	—
2A[a]	1.42(2)	2.15(1), 2.18(1)	2.27(1), 2.29(1)
2B[a]	1.42(2)	2.17(1), 2.16(1)	2.29(1), 2.29(1)
3	1.49(1)	2.179(8), 2.201(7)	2.251(7), 2.255(8), 2.265(7), 2.274(8)

[a] Two independent molecules in the unit cell.

Fig. 6. The $^{13}C\{^{1}H\}$ NMR spectrum (CO region) of **3** (^{13}CO enriched) in CH_2Cl_2–CD_2Cl_2 (4:1) at 21 and –90 °C, and at 90 °C in C_7D_8.

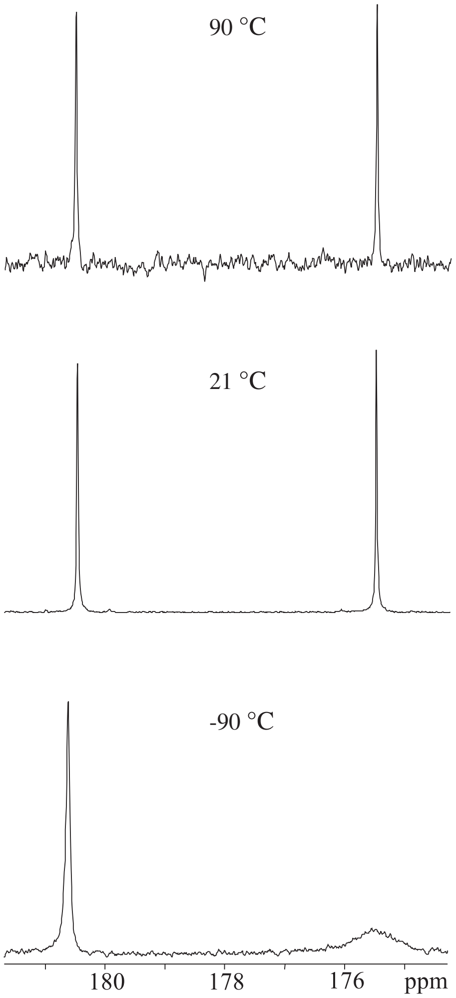

Scheme 2.

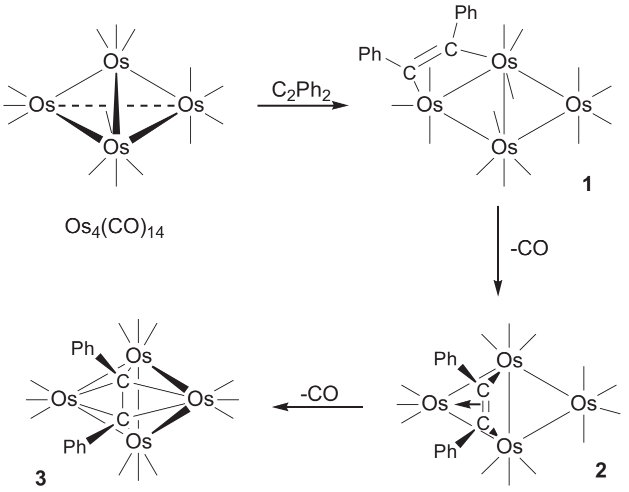

be different from uncoordinated C_2Ph_2 that may also result in enhanced reactivity of the coordinated alkyne.

The catalytic half-hydrogenation of alkynes to *cis*-alkenes is an important industrial process and is normally carried out with solid Pd catalysts that have been poisoned (e.g., Lindlar's catalyst) (40, 45). Some homogeneous half-hydrogenation catalysts are however known (46). The mechanism of the hydrogenation is not fully understood, but a mechanism that involves a dimetallacyclobutene unit appears to be an attractive possibility. Partial hydrogenation of the alkyne in the dimetallacyclobutene unit could take place by reaction with coordinated hydrogen (the Langmuir–Hinshelwood mechanism) or by direct attack by molecular H_2 (the Rideal mechanism) (38, 47).

The intermediacy of an organic substrate bound to two low-coordinate metal atoms on a surface may have more general applicability to the understanding of the action of site-specific surface catalysis. The precursory cluster $Os_4(CO)_{14}$ (that has a tetrahedral Os_4 nucleus) is prepared by pyrolysis of $Os_4(CO)_{15}$. The latter cluster has a planar structure and hence is a model for a metal surface. Both $Os_4(CO)_{14}$ and $Os_4(CO)_{15}$ have unusual bonding that is not found in higher nuclearity Os clusters (48, 49).

Some corners and imperfect edges of metal surfaces resemble these clusters. This is shown in Scheme 3 for a corner site; the active site is designated a "PT" (planar-tetrahedral) site. To allow the unique metal atom to hop from the planar to the tetrahedral site (Scheme 3) probably requires the atom not to be coordinated to a metal atom below the plane it originates from.

There would be more of these atoms the greater the surface area and in freshly prepared catalysts. It is a general observation for surface catalysts that they are usually more active the more finely divided they are and if they are freshly prepared (38). It may be that after the surface and step sites are saturated (i.e., analogous to **2** and **3**) there must be surface reformation in order for the PT sites to be activated. A ligand must also dissociate from the dangling atom to allow formation of the tetrahedral form of the PT site. Both steps might explain the lag time that some catalysts exhibit before catalysis begins (38). The model also explains why only certain metals are active and why bimetallic catalysts can be more active than catalysts comprised of the individual atoms (38). The metal atoms of the PT site have few metal–metal

Scheme 3.

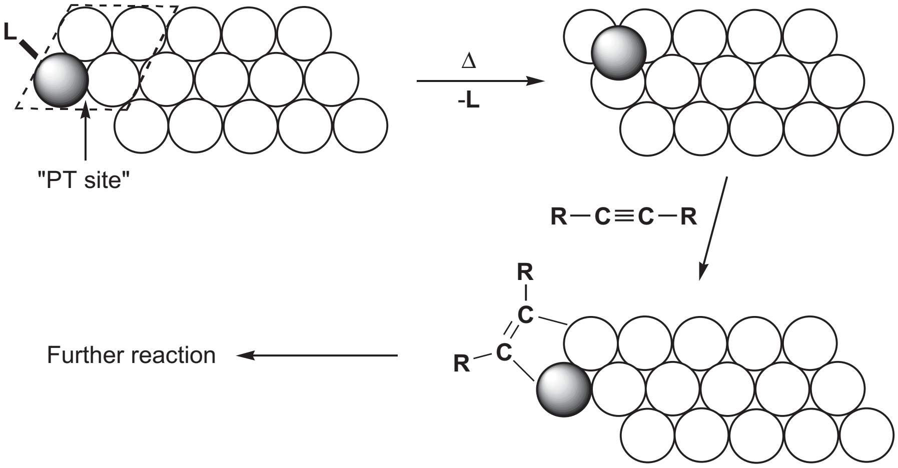

contacts and might be expected to have frontier orbitals like the corresponding metal atoms in mononuclear complexes. The most active metals for surface catalysts usually contain metal atoms that are present in the most active homogeneous mononuclear catalysts (e.g., Rh and Pd) (50). In the model, the substrate is bound to just two metal atoms and therefore it will have different susceptibilities to attack depending on whether it is coordinated to metals that are identical or different. Catalysts are often more effective with oxide promoters (38). If the atoms directly below or adjacent to the PT site were oxide ions, then the reactivity of the site would be strongly influenced by the ions.

Studies on the reactivity of clusters **1**–**3** (and derivatives thereof) with hydrogen and other small molecules are currently in progress.

Acknowledgements

We thank the Natural Sciences and Engineering Research Council of Canada (NSERC) for financial support.

References

1. (*a*) E. Sappa, A. Tiripiccio, and P. Braustein. Chem. Rev. **83**, 203 (1983); (*b*) P.R. Raithby and M.J. Rosales. Adv. Inorg. Radiochem. **29**, 169 (1985); (*c*) S. Deabate, R. Giordano, and E. Sappa. J. Cluster Sci. **8**, 407 (1997); (*d*) E. Sappa. J. Organomet. Chem. **573**, 139 (1999); (*e*) P.J. Low and M.I. Bruce. Adv. Organomet. Chem. **48**, 71 (2001).
2. Fe: (*a*) G. Wilkinson, F.G.A. Stone, and E.W. Abel (*Editors*). Comprehensive organometallic chemistry. Vol. 4. Pergamon, Oxford. 1982. Chap. 31.3–31.5; (*b*) G. Wilkinson, F.G.A. Stone, and E.W. Abel (*Editors*). Comprehensive organometallic chemistry II. Vol. 7. Pergamon, Oxford. 1995. Chap. 2–4; Some recent examples: (*c*) P.J. Low, A.J. Carty, K.A. Udachin, and G.D. Enright. J. Chem. Soc. Chem. Commun. 411 (2001); (*d*) A.J. Carty, G. Hogarth, G.D. Enright, J.W. Steed, and D. Georganopoulou. J. Chem. Soc. Chem. Commun. 1499 (1999).
3. Ru/Os: (*a*) G. Wilkinson, F.G.A. Stone, and E.W. Abel (*Editors*). Comprehensive organometallic chemistry. Vol. 4. Pergamon, Oxford. 1982. Chap. 32.3–32.6 and 33; (*b*) G. Wilkinson, F.G.A. Stone, and E.W. Abel (*Editors*). Comprehensive organometallic chemistry II. Vol. 7. Pergamon, Oxford. 1995. Chap. 8 and 13–16; Some recent examples: (*c*) M.I. Bruce, A.C. Meier, B.W. Skelton, A.H. White, and N.N. Zaitseva. Aust. J. Chem. **54**, 319 (2001); (*d*) R.L. Mallors, A.J. Blake, P.J. Dyson, B.F.G. Johnson, and S. Parsons. Organometallics, **16**, 1668 (1997); (*e*) M. Deng and W.K. Leong. Organometallics, **21**, 1221 (2002); (*f*) S.P. Tunik, V.D. Khripun, I.A. Balova, E. Nordlander, M. Haukka, T.A. Pakkanen, and P.R. Raithby. Organometallics, **20**, 3854 (2001); (*g*) J.A. Cabeza, I. del Río, P. García-Álverez, and D. Miguel. Organometallics, **24**, 665 (2005)
4. (*a*) V. Busetti, G. Granozzi, S. Aime, R. Gobetto, and D. Osella. Organometallics, **3**, 1510 (1984); (*b*) S. Brait, G. Gervasio, D. Marabello, and E. Sappa. J. Chem. Soc. Dalton Trans. 989 (2000); (*c*) E. Gatto, G. Gervasio, D. Marabello, and E. Sappa. J. Chem. Soc. Dalton Trans. 1448 (2002).
5. Recent examples: (*a*) P.J. Low, K.A. Udachin, and A.J. Carty. J. Cluster Sci. **15**, 1040 (2005); (*b*) P.J. Low, T.M. Hayes, K.A. Udachin, A.E. Goeta, J.A.K. Howard, D. Gary, and A.J. Carty. J. Chem. Soc. Dalton Trans. 1455 (2002); (*c*) M.I. Alcalde, A.J. Carty, Y. Chi, E. Delgado, B. Donnadieu, E. Hernandez, K. Dallmann, and J. Sanchez-Nieves. J. Chem. Soc. Dalton Trans. 2502 (2001); (*d*) P.J. Low, K.A. Udachin, G.D. Enright, and A.J. Carty. J. Organomet. Chem. **578**, 103 (1999); (*e*) P. Blenkiron, G.D. Enright, P.J. Low, J.F. Corrigan, N.J. Taylor, Y. Chin, J.-Y. Saillard, and A.J. Carty. Organometallics, **17**, 2447 (1998); (*f*) E. Delgado, Y. Chi, W. Wang, G. Hogarth, P.J. Low, G.D. Enright, S.-M. Peng, G.-H. Lee, and A.J. Carty. Organometallics, **17**, 2936 (1998); (*g*) P.J. Low, G.D. Enright, and A.J. Carty. J. Organomet. Chem. **565**, 279 (1998).
6. E. Sappa, A. Tiripicchio, A.J. Carty, and G.E. Toogood. Prog. Inorg. Chem. **35**, 437 (1987).
7. (*a*) M. Tachikawa, J.R. Shapley, and C.G. Pierpont. J. Am. Chem. Soc. **97**, 7172 (1975); (*b*) C.G. Pierpont. Inorg. Chem. **16**, 636 (1977);
8. (*a*) O. Gambino, G.A. Vaglio, R.P. Ferrari, and G. Cetini. J. Organomet. Chem. **30**, 381 (1971); (*b*) G. Ferraris and G. Gervasio. J. Chem. Soc. Dalton Trans. 1813 (1974); (*c*) A.J. Poë, D.H. Farrar, R. Ramachandran, and C. Moreno. Inorg. Chem. Acta, **274**, 82 (1998); (*d*) A.J. Poë and C. Moreno. Organometallics, **18**, 5518 (1999).
9. A.J. Poë, C.N. Sampson, and R.T. Smith. J. Am. Chem. Soc. **108**, 5459 (1986).
10. E. Rosenberg, J. Bracker-Novak, R.W. Gellert, S. Aime, R. Gobetto, and D. Osella. J. Organomet. Chem. **365**, 163 (1989).
11. A.J. Deeming. Adv. Organomet. Chem. **26**, 1 (1986).

12. (*a*) C.-Y. Lu, F.W.B. Einstein, V.J. Johnston, and R.K. Pomeroy. Inorg. Chem. **28**, 4212 (1989); (*b*) W. Wang, R.J. Batchelor, F.W.B. Einstein, C.-Y. Lu, and R.K. Pomeroy. Organometallics, **12**, 3598 (1993).
13. J.P. Canal, G.P.A. Yap, and R.K. Pomeroy. Organometallics, **22**, 3439 (2003).
14. R.F. Alex and R.K. Pomeroy. Organometallics, **41**, 2437 (1987).
15. J.P. Canal. Ph.D. thesis, Simon Fraser University, Burnaby, British Columbia. 2004.
16. M.R. Churchill and B.G. DeBoer. Inorg. Chem. **16**, 878 (1977).
17. G.R. John, B.F.G. Johnson, and J. Lewis. J. Organomet. Chem. **181**, 143 (1979).
18. For example: (*a*) H.B. Davis, F.W.B. Einstein, P.G. Glavina, T. Jones, R.K. Pomeroy, and P. Rushman. Organometallics, **8**, 1030 (1989); (*b*) F. Jiang, J.L. Male, K. Biradha, W.K. Leong, R.K. Pomeroy, and M.J. Zaworotko. Organometallics, **17**, 5810 (1998); (*c*) F. Jiang, H.A. Jenkins, K. Biradha, H.B. Davis, R.K. Pomeroy, and M.J. Zaworotko. Organometallics, **19**, 5049 (2000).
19. (*a*) D.M. Hoffman and R. Hoffmann. J. Chem. Soc. Dalton Trans. 1471 (1982); (*b*) M.R. Gagné and J. Takats. Organometallics **7**, 561 (1988); (*c*) A. Krebs, A. Jacobsen-Bauer, E. Haupt, M. Veith, and V. Huch. Angew. Chem. **101**, 640 (1989); (*d*) A.A. Cherkas, N. Hadj-Bagheri, A.J. Carty, E. Sappa, M.A. Pellinghelli, and A. Tiripicchio. Organometallics, **9**, 1887 (1990); (*e*) H.A. Mirza, J.J. Vittal, and R.J. Puddephatt. Organometallics, **13**, 3063 (1994); (*f*) C.P. Casey, W.T. Boese, R.S. Carino, and P.C. Ford. Organometallics, **15**, 2189 (1996); (*g*) C.P. Casey, R.S. Carino, H. Sakaba, and R.K. Hayashi. Organometallics, **15**, 2640 (1996); (*h*) H.A. Mirza, J.J. Vittal, and R.J. Puddephatt. J. Coord. Chem. **37**, 131 (1996); (*i*) S. Doherty, M. Waugh, T.H. Scanlan, M.R.J. Elsegood, and W. Glegg. Organometallics, **18**, 679 (1999).
20. M.C. Comstock and J.R. Shapley. Organometallics, **16**, 4816 (1997).
21. C.P. Casey, R.S. Carino, R.K. Hayashi, and K.D. Schladetzky. J. Am. Chem. Soc. **118**, 1617 (1996).
22. P.F. Heveldt, B.F.G. Johnson, J. Lewis, P.R. Raithby, and G.M. Sheldrick. J. Chem. Soc. Chem. Commun. 340 (1978).
23. M.R. Burke and J. Takats. Organomet. Chem. **302**, C25 (1986).
24. O.P. Anderson, B.R. Bender, J.R. Norton, A.C. Larson, and P.J. Vergamini. Organometallics, **10**, 3145 (1991).
25. B.E. Mann and B.F. Taylor. ^{13}C NMR data for organometallic compounds. Academic Press, New York. 1981.
26. B.F.G. Johnson, J Lewis, P.R. Raithby, and M.J. Rosales. J. Chem. Soc. Dalton Trans. 2645 (1983).
27. D. Braga, F. Grepioni, B.F.G. Johnson, J. Lewis, and J.A. Lunniss. J. Chem. Soc. Dalton Trans. 1101 (1992).
28. C.R. Eady, W.G. Jackson, B.F.G. Johnson, J. Lewis, and T.W. Matheson. J. Chem. Soc. Chem. Commun. 958 (1975).
29. B.F.G. Johnson, J. Lewis, M.-A. Pearsall, and L.G. Scott. J. Organomet. Chem. **413**, 337 (1991).
30. C.R. Eady, B.F.G. Johnson, J. Lewis, R. Mason, P.B. Hitchcock, and K.M. Thomas. J. Chem. Soc. Chem. Commun. 385 (1977).
31. V.M. Hansen, R.J. Batchelor, F.W.B Einstein, J.L. Male, and R.K. Pomeroy. Organometallics, **16**, 4875 (1997).
32. B.F.G Johnson, J. Lewis, B.E. Reichert, K.T. Schorpp, and G.M. Sheldrick. J. Chem. Soc. Dalton Trans. 1417 (1977).
33. (*a*) H. Bantel, B. Hansert, A.K. Powell, M. Tasi, and H. Vahrenkamp. Angew. Chem. Int. Ed. Engl. **28**, 1059 (1989); (*b*) H. Chen, B.F.G. Johnson, J. Lewis, and P.R. Raithby. J. Chem. Soc. Chem. Commun. 373 (1990); (*c*) G. Chen, M. Deng, C.H. Lee, and W.K. Leong. Organometallics, **21**, 1227 (2002).
34. R. Jackson, B.F.G Johnson, J. Lewis, P.R. Raithby, and S.W. Sankey. J. Organomet. Chem. **193**, C1 (1980).
35. J. Sanchez-Nieves, B.T. Sterenberg, K.A. Udachin, and A.J. Carty. Can. J. Chem. **82**, 1507 (2004).
36. (*a*) E.L. Muetterties. Bull. Soc. Chim. Belg. **84**, 959 (1975); (*b*) E.L. Muetterties, T.N. Rhodin, E. Band, C.F. Brucker, and W.R. Pretzer. Chem. Rev. **79**, 91 (1979).
37. E.L. Muetterties, W.R. Pretzer, M.G. Thomas, B.F. Beier, D.L. Thorn, V.W. Day, and A.B. Anderson. J. Am. Chem. Soc. **100**, 2090 (1978).
38. G.A. Somorjai. Introduction to surface chemistry and catalysis. Wiley, New York. 1994.
39. (*a*) G.A. Somorjai and M. Yang. Top. Catal. **24**, 61 (2003); (*b*) G.A. Somorjai. J. Phys. Chem. B, **106**, 9201 (2002); (*c*) P.S. Cremer, X. Su, Y.R. Shen, and G.A. Somorjai. J. Am. Chem. Soc. **118**, 2942 (1996); (*d*) G.A. Somorjai. J. Phys. Chem. B, **106**, 9201 (2002).
40. G.V. Smith and F. Notheisz. Heterogeneous catalysis in organic chemistry. Academic Press, San Diego. 1999.
41. C.R. Henry. Surf. Sci. Rep. **31**, 231(1998).
42. (*a*) A.M. Doyle, S.K. Shaikhutdinov, S.D. Jackson, and H.-J. Freud. H. Angew. Chem. Int. Ed. **42**, 5240 (2003); (*b*) V. Johánek, S. Schauermann, M. Laurin, J. Libuda, and H.-J. Freund. Angew. Chem. Int. Ed. **42**, 3035 (2003).
43. (*a*) J. Wei and E. Iglesia. J. Phys. Chem. B, **108**, 4094 (2004); (*b*) J. Wei and E. Iglesia. J. Catal. **225**, 116 (2004).
44. J. Wei and E. Iglesia. J. Phys. Chem. B, **108**, 7253 (2004).
45. J.G. Ulan, W.F. Maier, and D.A. Smith. J. Org. Chem. **52**, 3132 (1987).
46. For example: (*a*) J.A. Cabeza, I. del Río, J.M. Fernández-Colinas, and V. Riera. Organometallics, **15**, 449 (1996); (*b*) R. Giordano, E. Sappa, and S.A. Knox. J. Cluster Sci. **7**, 179 (1996).
47. M. Farina, C. Morandi, E. Mantica, and D. Botta. J. Chem. Soc. Chem. Commun. 816 (1976).
48. (*a*) F.W.B. Einstein, V.J. Johnston, A.K. Ma, and R.K. Pomeroy. Can. J. Chem. **73**, 1223 (1995); (*b*) V.J. Johnston, F.W.B. Einstein, and R.K. Pomeroy. J. Am. Chem. Soc. **109**, 7220 (1987).
49. V.J. Johnston, F.W.B. Einstein, and R.K. Pomeroy. Organometallics, **7**, 1867 (1988).
50. (*a*) D.D. Shriver, H.D. Kaesz, and R.D. Adams (*Editors*). The chemistry of metal clusters. VCH, New York. 1990; (*b*) B.C. Gates, L. Guczi, and H. Knözinger (*Editors*). Metal clusters in catalysis. Elsevier, Amsterdam. 1986.